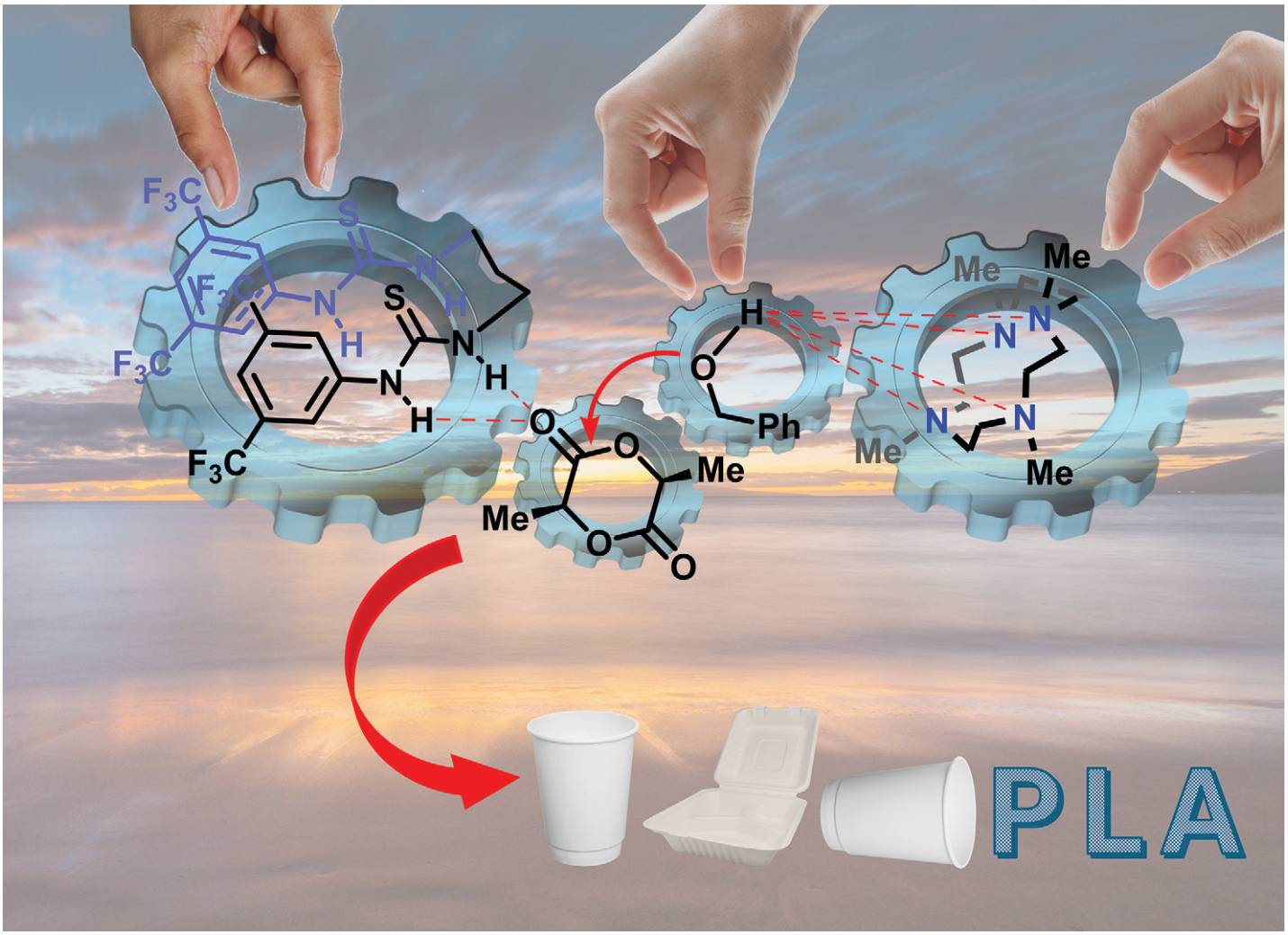


Showcasing research from Professor Mazzeo and Della Sala's laboratories, Department of Chemistry and Biology "A. Zambelli", University of Salerno, Italy.

Bis-thiourea and macrocyclic polyamines as binary organocatalysts for the ROP of lactide

Co-operation may be the secret of success in catalysis. Bicomponent organic catalysts formed by bis-thiourea and macrocyclic polyamines proved efficient binary organocatalysts for the ROP of lactide. The synergy among the nitrogen atoms of polyamines in the activation of the hydroxyl group of the polymeric growing chain, favoured by opportune architectures of the macrocyclic, proved crucial for effective catalysis.

As featured in:



See Lucia Caporaso, Giorgio Della Sala, Mina Mazzeo *et al.*, *Catal. Sci. Technol.*, 2025, **15**, 71.

ROYAL SOCIETY OF CHEMISTRY

rsc.li/catalysis

Registered charity number: 207890

Catalysis Science & Technology

ROYAL SOCIETY OF CHEMISTRY

PAPER

View Article Online
View Journal | View Issue

Check for updates

Cite this: *Catal. Sci. Technol.*, 2025, **15**, 71

Bis-thiourea and macrocyclic polyamines as binary organocatalysts for the ROP of lactide†

Assunta D'Amato, ‡[a] Maria Voccia,‡[b] Filippo Bruno,[a] Sara D'Aniello,[a] Lucia Caporaso,*[a] Francesco De Riccardis,[a] Irene Izzo,[a] Giorgio Della Sala *[a] and Mina Mazzeo *[a]

New binary catalysts formed by 1,1′-(propane-1,3-diyl)bis(3-(3,5-bis(trifluoromethyl)phenyl)thiourea) and a series of specifically designed flexible polyaza-macrocycles, prepared by a convenient iterative solid-phase synthesis and reduction, have been investigated for the ring opening polymerization (ROP) of L-lactide. These systems, in the presence of benzyl alcohol as initiator, showed high activity, delivering polylactides with high chain-end fidelity and controlled molecular weights with narrow dispersities. A detailed study of the structure–activity relationship for various polyaza-macrocycles, with different sizes and *N*-side chains, was performed. The best results were exhibited by cyclen derivatives, improving the performances achieved by the well-established triazacyclononane (TACN) co-catalyst. DFT (density functional theory) calculations, performed on each putative polyazamacrocycle/benzyl alcohol complex, assessed both the ring size and the *N*-alkyl steric hindrance roles on the initiator activation, providing a rationale for the activity scale experimentally observed for macrocyclic polyamines.

Received 1st August 2024,
Accepted 26th September 2024

DOI: 10.1039/d4cy00952e

rsc.li/catalysis

Open Access Article. Published on 27 September 2024. Downloaded on 1/28/2025 3:02:08 PM.
This article is licensed under a Creative Commons Attribution-NonCommercial 3.0 Unported Licence.

Introduction

In the last two decades, organocatalytic ring-opening polymerization (ROP) of various monomers, such as cyclic esters,[1–3] epoxides in combination with CO_2 (ref. 4–6) or anhydrides,[7–11] and *N*-carboxy anhydrides,[12] has emerged as an attractive route for the synthesis of functional, biocompatible, and biodegradable materials.[13–16]

The high functional group tolerance of many organic catalysts and their ability to efficiently control macromolecular parameters, such as the structure of chain end groups as well as the molecular masses and their distribution, have provided new opportunities for macromolecular synthesis and design.[11,17–20]

Moreover, organic catalysts offer the additional advantage of lower toxicity and ease of removal in comparison to many metal-based catalysts, representing valuable tools to produce polymeric materials for biomedical and food packaging applications.

Different families of organocatalysts have been effectively employed in ROP, including Brønsted/Lewis acids and bases such as amines,[21–24] ureas,[25–27] phosphoric acids,[28] phosphazenes,[2,10,29] and N-heterocyclic carbenes (NHCs).[30–32]

In particular, bicomponent catalysts formed by an H-bond donating (thio)urea in combination with an H-bond accepting organic base are among the most efficient organocatalysts for the ROP of cyclic esters and carbonates.[16,26,27,33]

In the presence of alcohol initiators, they generate bifunctional cooperative systems where the amine base was proposed to serve as the H-bond acceptor, activating the alcohol in the initiation step (and the alcoholic growing chain during propagation), while the Lewis acidic thiourea activates the monomer.[26]

Specifically, bis-(thio)ureas, as H-bond donating co-catalysts, revealed enhanced catalytic activity in comparison to the related mono-(thio)ureas in the ROP of L-lactide, thanks to the autoactivation phenomena between the (thio)urea pockets (Fig. 1).[34]

The cooperative mechanism reaches its maximum efficiency when the pK_a of the base and (thio)urea are closely matched.[21] A strategy adopted for the amplification of catalytic activity is to expand the number of basic amine sites.

In their recent studies, Coady and Hedrick[35] demonstrated that polyamines characterized by a N–N interatomic distance close to 3.0 Å, and an orientation angle of their respective lone pairs close to 50°, are the most efficient bases to promote this process and at the same time suppressing

[a] *Dipartimento di Chimica e Biologia "Adolfo Zambelli", University di Salerno, via Giovanni Paolo II, 132, 84084 Fisciano, SA, Italy. E-mail: lcaporaso@unisa.it, gdsala@unisa.it*
[b] *Dipartimento di Scienza dei Materiali, Università di Milano-Bicocca, via R. Cozzi, 55, I-20125 Milano, Italy*

† Electronic supplementary information (ESI) available. See DOI: https://doi.org/10.1039/d4cy00952e

‡ The authors have contributed equally to this work.

Open Access Article. Published on 27 September 2024. Downloaded on 1/28/2025 3:02:08 PM.
This article is licensed under a Creative Commons Attribution-NonCommercial 3.0 Unported Licence.

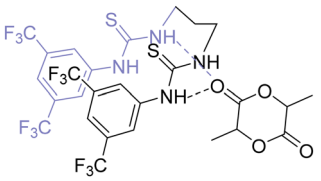


Fig. 1 Possible mode of bis-thiourea activation.

deleterious transesterification reactions. Such structural features enable chelative association of the nitrogen atoms with the hydroxyl proton of the alcohol initiator as well as of the growing chain, enhancing OH nucleophilicity toward the incoming monomer. Molecules that were found to combine these principles were sparteine and 1,4,7-trimethyl-1,4,7-triazacyclononane (**Me$_3$TACN**), in which the reduced conformational freedom properly pre-orients the nitrogen atom lone pairs for the activation of the hydroxyl group. Despite the high potentials of cyclic polyamines as the Lewis base of bicomponent organocatalysts, a systematic study of the effect of their structural modifications on the catalytic activity has never been carried out.

Recently, we introduced a convenient method to prepare polyaza-macrocycles with different ring sizes and side chains through reduction of the corresponding cyclic oligoamides, readily accessible through solid-phase synthesis.[36]

Inspired by the above considerations, in this work we decided to investigate the behaviour of different size polyamine macrocycles, bearing benzyl or methyl substituents (Fig. 2), in combination with the bis-thiourea **bTU** as catalysts for the polymerization of L-lactide (L-LA).

The number of nitrogen donor sites, the nature of different substituents and the conformational flexibility of the polyaza-macrocycles are parameters that have been screened to elucidate their effect on the catalytic activity. For our comparative studies, the bis-thiourea **bTU** was selected as the H-bond donating co-catalyst, since it showed enhanced catalytic activity compared to the related mono-thiourea in the ROP of L-lactide.[34,37] DFT studies were also performed to rationalize the effect of the structural modifications of cyclic polyamines on their catalytic behaviour.

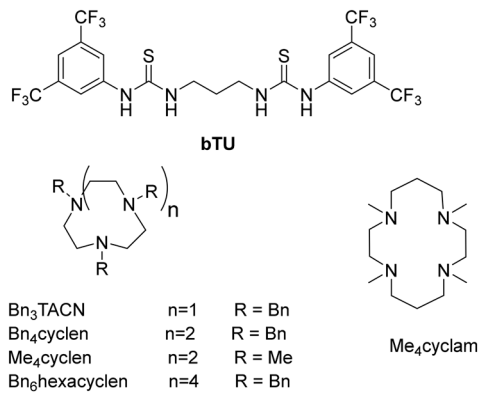


Fig. 2 Structures of the bis-thiourea and macrocyclic polyamine catalysts.

Experimental

Materials and methods

Moisture and air-sensitive materials were manipulated under nitrogen using Schlenk techniques or an MBraun Labmaster glovebox. The used glassware was dried in an oven at 120 °C and subsequently subjected to vacuum-nitrogen cycles. Toluene and methanol were refluxed over Na and distilled under nitrogen. Tetrahydrofuran (THF) was refluxed over Na and benzophenone and distilled under nitrogen. Deuterated solvents were purchased from Sigma-Aldrich and dried over activated 3 Å molecular sieves prior to use.

All the reagents used for the synthesis of the compounds and 1,3-diaminopropane, 3,5-bis(trifluoromethyl)phenyl isothiocyanate were purchased from Sigma-Aldrich Merck. All the other reagents and solvents were purchased from Sigma-Aldrich Merck and used without further purification.

Instruments and measurements

NMR spectroscopy. NMR spectroscopy of polymers were performed in deuterated solvents at room temperature on Bruker Avance 300, 400 or 600 spectrometers (^{1}H: 300.13, 400.13, 600.13 MHz; ^{13}C: 75.47, 100.62, 150.92 MHz, respectively). The resonances are reported in ppm (δ) and are referenced to the residual solvent peak at δ = 7.16 ppm for C_6D_6 and δ = 7.27 for $CDCl_3$. Spectra recording was performed using Bruker-TopSpin v2.1 software. Data processing was performed using TopSpin v2.1 or MestReNova v6.0.2 software.

Gel Permeation Chromatography (GPC). Molecular masses (M_n and M_w) and their dispersities ($Đ$) were measured by GPC. The measurements were performed at 30 °C on a Waters 1525 binary system equipped with a Waters 2414 refractive index (RI) detector and a Waters 2487 dual λ absorption (UV, λ_{abs} = 220 nm) detector, using tetrahydrofuran as the eluent (1.0 mL min^{-1}) and employing a system of four Styragel HR columns (7.8 × 300 mm; range 103–106 Å). Narrow polystyrene standards were used as reference and Waters Breeze v3.30 software was used for data processing. When $CHCl_3$ was used as the solvent, Styragel HR3 columns and Styragel HR4 columns were used.

Differential Scanning Calorimetry (DSC). The melting points (T_m) and enthalpy of fusion (ΔH_m) of the polymer samples were measured by using aluminum pans and a DSC 2920 TA Instruments apparatus, calibrated with indium. Measurements were performed under nitrogen flow with a heating rate of 10 °C min^{-1} in the range of −80 to +220 °C. DSC data were processed with TA Universal Analysis v2.3 software and are reported for the second heating cycle.

MALDI-ToF analysis. Mass spectra were recorded using a Bruker solariX XR Fourier transform ion cyclotron resonance (FT-ICR) mass spectrometer (Bruker Daltonik GmbH, Bremen, Germany) equipped with a 7 T refrigerated actively

 This journal is © The Royal Society of Chemistry 2025

Open Access Article. Published on 27 September 2024. Downloaded on 1/28/2025 3:02:08 PM. This article is licensed under a Creative Commons Attribution-NonCommercial 3.0 Unported Licence.

shielded superconducting magnet (Bruker Biospin, Wissembourg, France). The samples were prepared at a concentration of 1.0 mg mL^{-1} in THF, while the matrix (DCTB) was mixed at a concentration of 10.0 mg mL^{-1}.

Computational details. All the DFT geometry optimizations of the conformers and adducts were performed at the GGA BP86 (ref. 38–40) level with the Gaussian09 package.[41] The electronic configuration of the systems and the reported free energies were described with the 6-31G basis set for all the atoms.[42] All geometry optimizations were characterized as minimum through frequency calculations and were performed without symmetry constraints. Solvent effects were estimated with the PCM model[43,44] using CH_2Cl_2 as the solvent. The reported free energies were built through single point energy calculations on the (BP86/6-31G) geometries using the M06 functional[45] and the triple-ζ TZVP basis sets.[46] These frequencies were used to calculate unscaled zero-point energies (ZPEs) as well as thermal corrections and entropy effects at 298.15 K and 1 atm. Finally, the D3 Grimme pairwise scheme to account for dispersion corrections was considered for the energies' calculations, but no considerable electronic factor was found.[47]

Synthetic procedures

Synthesis of 1,1′-(propane-1,3-diyl)bis(3-(3,5-bis(trifluoromethyl) phenyl)thiourea). A dried 100 mL Schlenk flask was charged with a stir bar, dry benzene (4.0 mL) and 1,3-diaminopropane (0.154 mL, 1.84 mmol). 3,5-Bis(trifluoromethyl)phenyl isothiocyanate (0.674 mL, 3.68 mmol) was added dropwise to the round bottom flask. The solution was stirred for 24 hours at room temperature, and after this time the solid was recovered by filtration, washed with hexane and then dried *in vacuo* for 5 hours. The final product (0.65 g, yield: 58%) was characterized by ^{1}H, ^{13}C and ^{19}F NMR spectroscopy. The spectra are reported in the ESI† (Fig. S1–S4).

Synthesis of polyaza-macrocycles. Polyaza-macrocycles were prepared following the general procedure described in the literature and the ^{1}H NMR spectra overlapped those reported.[36,48,49]

Me_4cyclen[50] and **Me_4cyclam**[51] were obtained from commercially available cyclen and cyclam respectively, as previously described in the literature.

Bn_3TACN:[36] ^{1}H NMR (400 MHz, $CDCl_3$) δ: 7.40–7.30 (15H, m), 5.54 (3H, d, J 14.4 Hz), 4.58 (3H, d, J 15.5 Hz), 4.21 (3H, d, J 14.4 Hz), 3.73 (3H, d, J 15.5 Hz).

Bn_4cyclen:[36] ^{1}H NMR (600 MHz, $CDCl_3$) δ: 7.32–7.08 (20H, m), 5.56 (2H, d, J 14.4 Hz), 5.41 (2H, d, J 14.9 Hz), 4.45 (2H, d, J 17.2 Hz), 4.38 (2H, d, J 17.2 Hz), 4.34 (2H, d, J 17.2 Hz), 3.74 (2H, d, J 14.4 Hz), 3.50 (2H, d, J 14.9 Hz), 3.49 (2H, d, J 17.2 Hz).

Bn_6hexacyclen:[36] ^{1}H NMR (400 MHz, $CDCl_3$, complex mixture of rotamers) δ: 7.40–7.04 (30H, m), 4.86–3.25 (24H, m).

Me_4cyclen:[52] ^{1}H-NMR (400 MHz, $CDCl_3$) δ: 2.20 (12H, s), 2.49 (16H, s).

Me_4cyclam:[51] ^{1}H NMR (400 MHz, $CDCl_3$) δ: 1.64 (4H, q, J 7 Hz), 2.20 (12H, s), 2.43 (16H, m).

Results and discussion

Polymerization of lactide

Initially, *N*-benzyl polyaza-macrocycles (n = 3, 4, 6, Fig. 2), in combination with one equivalent of bis-thiourea **bTU**, were selected to investigate the effect of the size of the macrocycle on the catalytic activity in the polymerization of L-lactide (Scheme 1).

The polymerization tests were performed in CH_2Cl_2 (1 M) at 25 °C with 2.5% catalyst loading of macrocyle/**bTU**, using benzyl alcohol as initiator. The isolated polymers were characterized by ^{1}H NMR, GPC and MALDI-ToF-MS analysis. Representative results are reported in Table 1.

At a monomer-to-initiator ratio of 100 ([L-LA]/[BnOH] = 100), a 44% conversion of lactide was achieved after 6 min (run 1, Table 1). The activity showed by **Bn_3TACN/bTU** was lower than that previously reported with the commercial cyclic amine 1,4,7-trimethyl-1,4,7-triazacyclononane (**Me_3TACN**). **Me_3TACN** gave, under the same reaction conditions, 89% conversion of the monomer.[34]

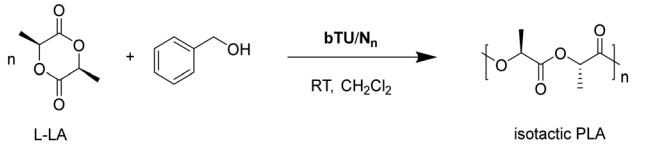
The reduced activity of **Bn_3TACN/bTU** was tentatively attributed to the higher steric hindrance created by the benzyl groups on the nitrogen atoms in comparison to the methyl groups of the **Me_3TACN.**

Gratifyingly, under the same reaction conditions, **Bn_4cyclen/bTU** led to quantitative conversion of the monomer after 6 minutes (run 2, Table 1), showing a higher activity than triazacyclononanes.

This could be a consequence of reduced steric encumbrance due to the larger dimension of the macrocycle and/or to a higher basicity of the cyclen structure because of the presence of an additional H-bond acceptor nitrogen atom.

Interestingly, when the larger **Bn_6hexacyclen** was tested under the same reaction conditions, no conversion of L-LA was observed (run 3, Table 1), even after prolonged times (24 hours).

The study proceeded halving the amount of catalyst (L-LA : polyaza-macrocycles : **bTU** = 80 : 1 : 1) and of the alcohol initiator (in amounts comparable to those used for metal catalysts). Both systems remained highly effective at lower concentrations, and the trend of activity previously observed between the two catalysts was maintained (runs 4 and 5, Table 1), confirming **Bn_4cyclen/bTU** as the best catalyst (with good conversion after only 30 min and full conversion after



Scheme 1 Polymerization of L-lactide (L-LA) by different size polyazamacrocycles (Nn)/**bTU**.

Open Access Article. Published on 27 September 2024. Downloaded on 1/28/2025 3:02:08 PM.
This article is licensed under a Creative Commons Attribution-NonCommercial 3.0 Unported Licence.

Table 1 Polymerization of L-lactide by polyaza-macrocycles (N_n) and **bTU**

Run[a]	N_n	Solvent	t (min)	Conv[c] (%)	M_{nGPC}[d] (kDa)	M_n^{the} (kDa)	$Đ$[d]
1	**Bn$_3$TACN**	CH_2Cl_2	6	44	5.9	6.3	1.17
2	**Bn$_4$cyclen**	CH_2Cl_2	6	95	12.2	13.7	1.14
3	**Bn$_6$hexacyclen**	CH_2Cl_2	30	—	—	—	—
4[b]	**Bn$_3$TACN**	CH_2Cl_2	30	13	7.4	3.0	1.14
5[b]	**Bn$_4$cyclen**	CH_2Cl_2	30	50	13.5	14.4	1.11
6[b]	**Bn$_4$cyclen**	CH_2Cl_2	75	>99	29.7	28.8	1.13
7[f]	**Bn$_4$cyclen**	CH_2Cl_2	75	98	26.3	28.2	1.12
8	**Bn$_4$cyclen**	THF	30	2	—	—	—
9[g]	**Bn$_4$cyclen**	Toluene	30	—	—	—	—
10	**Me$_4$cyclen**	CH_2Cl_2	2	94	24.5	27.1	1.07
11	**Me$_4$cyclam**	CH_2Cl_2	2	40	11.5	9.8	1.07

[a] All reactions, except run 4 and 5, were conducted at 25 °C with [L-LA] = 1 M, CH_2Cl_2 = 0.7 mL, N_n = **bTU** = 17.5 μmol; BnOH 7 μmol. [b] N_n = **bTU** = 8.8 μmol; BnOH 3.5 μmol. [c] Conversions of LA were determined by ^{1}H NMR. [d] Experimental M_{nGPC} (kDa) (corrected using factor of 0.58) and $Đ$ values were determined by GPC analysis using polystyrene standards. [e] M_n^{th} (g mol^{-1}) = MMLA × ([monomer]$_0$/[BnOH]$_0$) × LA conversion. [f] [*rac*-LA] = 1 M. [g] T = 80 °C.

90 min). The same activity was observed with the racemic substrate *rac*-LA (run 7, Table 1).

The solvent optimization runs (entries 6 and 7, Table 1) demonstrated the effect of the medium on the reactions. When the selected solvent changes from dichloromethane to THF or toluene, the catalytic activity of **Bn$_4$cyclen/bTU** was suppressed, and no conversion was observed even after prolonged reaction times and at temperatures up to 80 °C. These results are not surprising, considering the impact of the solvent on the hydrogen bonding interactions involved in the activation of both the monomer and the alcohol.[53,54] In this respect, THF may compete with the monomer in the coordination to the thiourea, whereas the poor conversion achieved in nonpolar toluene is possibly due to its tendency to stabilize an unreactive thiourea-polyamine complex.[55,56]

More mechanistic information was provided by kinetic studies performed on both the catalytic systems **Bn$_3$TACN/bTU** and **Bn$_4$cyclen/bTU** in CD_2Cl_2 at 25 °C. The conversions of the monomer were monitored by ^{1}H NMR spectroscopy for individual runs at different intervals. For both systems, L-LA polymerizations obeyed first-order kinetics in the monomer with instantaneous initiation (Fig. 3).

The apparent kinetic constants were 5.1 × 10^{-3} min^{-1} and 8.9 × 10^{-3} min^{-1} for **Bn$_3$TACN** and **Bn$_4$cyclen** respectively, and they well correlated with the activities observed in the polymerization runs reported in Table 1.

The results obtained suggest that the catalytic activity is strongly dependent on the size of the macrocycle and the type of *N*-alkyl groups.

As regards to the role of alkyl substituents, their steric hindrance seems to compromise the performance of the base.

To confirm this observation, we purposely synthetized the **Me$_4$cyclen** macrocycle in which the benzyl groups were substituted by the less sterically encumbered methyl groups.

To our pleasure, under the same polymerization conditions described in run 5, the catalytic system **Me$_4$cyclen/bTU** was significantly more active than **Bn$_4$cyclen/bTU** (compare run 8 and run 5, Table 1), as the quantitative conversion of the monomer was achieved after only 2 min, preserving the high ability in controlling the molecular masses of the produced polymer.

Finally, a larger cyclic polyamine, namely 1,4,8,11-tetramethyl-1,4,8,11-tetraazacyclotetradecane (**Me$_4$cyclam**), was synthetized. In this case the activity of **Me$_4$cyclam/bTU** was slightly lower than that obtained with **Bn$_4$cyclen/bTU** (see runs 9 and 5, Table 1).

Probably the longer propylene bridge between adjacent nitrogen atoms and the consequent higher macrocyclic conformational freedom less effectively meets the structural requirements for chelation of the hydroxyl protons of the propagating species.

All the polymerizations described exhibited an efficient control of the molecular masses: the experimental values were close to the theoretical ones with dispersities ($Đ$) lower than 1.14 (Fig. S10 and S11†). The characteristics of a living polymerization were also evidenced by the linear correlation

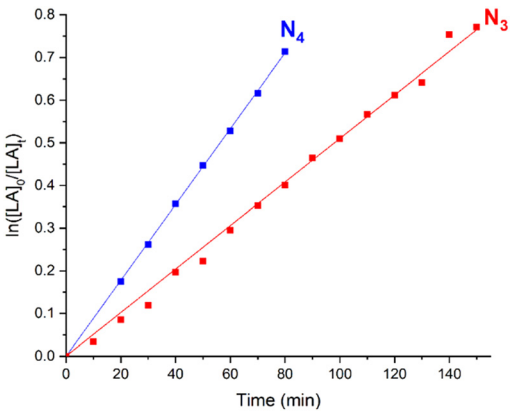


Fig. 3 Kinetic plot for ROP of L-LA promoted by **Bn$_3$TACN/bTU** (N_3) and **Bn$_4$cyclen/bTU** (N_4) depicting a reaction order of unity with respect to the monomer concentration. Pseudo first-order rate constants are: k_{app} = 0.0051 min^{-1} (R^2 = 0.998) for **Bn$_3$TACN** and k_{app} = 0.0089 min^{-1} for **Bn$_4$cyclen** (R^2 = 0.997).

This journal is © The Royal Society of Chemistry 2025

Open Access Article. Published on 27 September 2024. Downloaded on 1/28/2025 3:02:08 PM.
This article is licensed under a Creative Commons Attribution-NonCommercial 3.0 Unported Licence.

between M_n (measured by ^{1}H NMR) and monomer conversion (see Table S1†).

The initiation efficiency was investigated by ^{1}H NMR analysis of the end-groups of a low molecular weight PLA initiated by benzyl alcohol (run 2, Table 1). The only end-groups observed were the benzyl ester from the initiating alcohol and the ω-hydroxyl chain-ends, which is indicative of one molecule of initiator per polymer chain (Fig. S7†). In fact, the M_n^{th} evaluated by NMR was coherent with the value experimentally measured (10.5 kDa).

Analogously, the matrix-assisted laser desorption/ionization time-of-flight mass spectroscopy (MALDI-ToF MS) analysis showed a symmetric distribution of peaks associated to a single population of polymeric chains (δ m/z = 144) initiated by benzyl alcohol (Fig. 4). The absence of peak multiples of 72 m/z suggests that no post-polymerization transesterification is occurring.

The selectivity of these catalytic systems was also evident in the lack of any observable epimerization of the polylactides. Homonuclear decoupled ^{1}H NMR (Fig. S8†) and ^{13}C NMR spectra of PLA samples show only one resonance in the methine region, suggesting that the configuration of the monomer is retained in the polymerization. Thermal analysis performed by DSC on the PLAs produced in runs 1–4 revealed them to be highly isotactic with a melting point (T_m) of 170 °C (Fig. S5a and S6†).

The analysis of the sample obtained for racemic lactide by homonuclear decoupled ^{1}H NMR spectroscopy revealed an atactic microstructure Fig. S9.†

DFT calculations

For the described systems, a bimolecular hydrogen bond activation of both the monomer and the initiating/propagating alcohol was supposed to be active, in analogy with the previously reported studies.[46]

With the aim to rationalize the experimentally observed relative activity, the interaction between the benzyl alcohol and the polyaza-macrocycles was studied by DFT calculations.[26] The species investigated, TACN, cyclen and hexacyclen, bear benzyl or methyl substituents, as described in Fig. 5.

As reported in the literature,[35] the activation of initiating/propagating alcohol by amine compounds originates from a chelative association of the hydroxyl proton of the alcohol with the amine nitrogen atoms of the macrocycle. The cooperation between the nitrogen atoms in the coordination is known to play a crucial role, making the oxygen of the alcohol more nucleophilic and, consequently, more reactive.[21]

This cooperation takes place when the rigid macrocycle structure adopts a stable conformation showing N–N distances of about 3 Å with lone pairs oriented around 44° above the N–N plane.[35]

Looking to triazamacrocycles, we performed calculations on **Me$_3$TACN/Alcohol** and **Bn$_3$TACN/Alcohol** complexes starting from the corresponding macrocycle and benzyl alcohol at infinite distance.

Calculations showed that the adduct is in a thermodynamic equilibrium with the reagents for both **Me$_3$TACN/Alcohol** and **Bn$_3$TACN/Alcohol** since ΔG is 0.3 kcal mol^{-1} and 1.5 kcal mol^{-1}, respectively (see Fig. 6).

Previously reported X-ray analysis of Na^+ and H^+ complexes of **Bn$_3$TACN** and **Bn$_4$cyclen** in the solid state revealed "closed" structures, with the *N*-benzyl moieties arranged almost perpendicularly to the mean plane of the macrocycle wrapping around the cation.[36] In contrast, calculations show that on the respective benzyl alcohol adduct, the benzyl rings move on a parallel plane ("open" geometry) minimizing steric repulsions and allowing the hydroxyl proton to interact with greater extent with the nitrogen atoms of the macrocycle. In fact, for **Bn$_3$TACN**, this "open" geometry is about 2.0 kcal mol^{-1} more stable than the "closed" one (see Fig. 7).

In analogy to what already reported for **Me$_3$TACN**, showing a N–N distance of 2.96 Å and an orientation angle between H···N···N atoms of 55° and 42°,[35] the calculations show that for **Bn$_3$TACN/Alcohol Open**, the distance calculated between two adjacent nitrogen atoms (2.98 Å) and the angles between the H atom of alcohol and the two involved N atoms (53° and 45°) were values useful to favour an effective interaction.

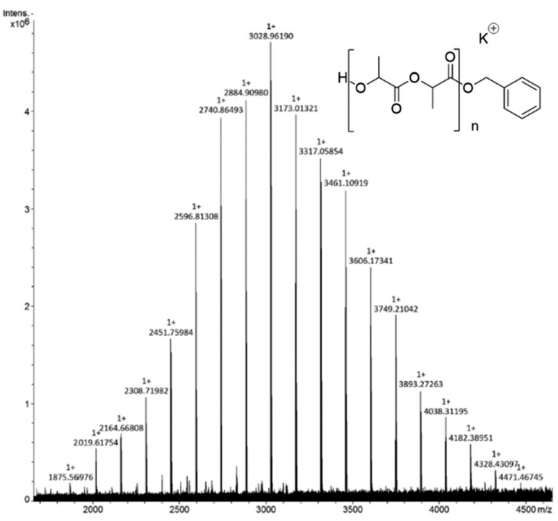


Fig. 4 MALDI-ToF-MS spectrum of PLA obtained with 20 equivalents of L-LA under reaction conditions described in run 1.

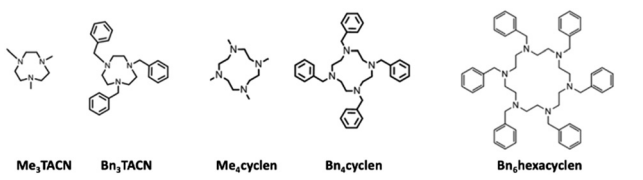


Fig. 5 Schematic structures of the different polyaza-macrocycles investigated.

Open Access Article. Published on 27 September 2024. Downloaded on 1/28/2025 3:02:08 PM.
This article is licensed under a Creative Commons Attribution-NonCommercial 3.0 Unported Licence.

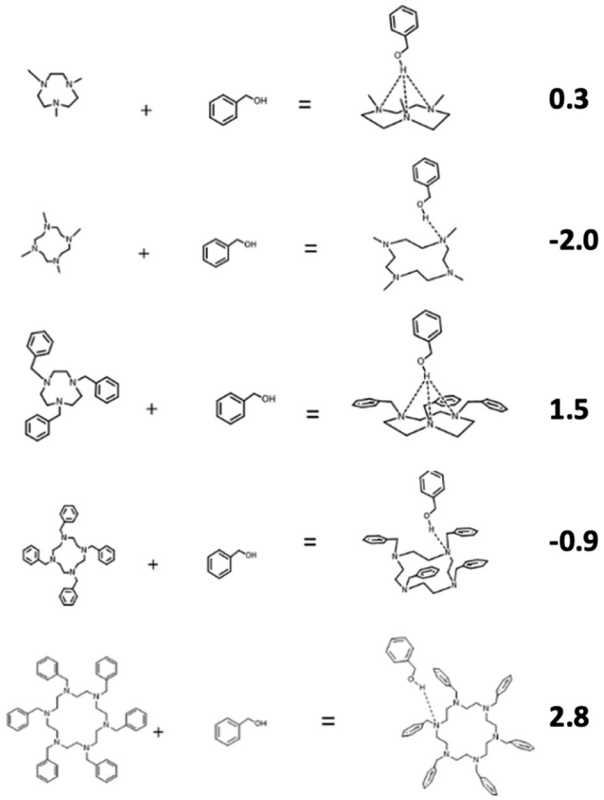


Fig. 6 Free energies (kcal mol^{-1}) of the adduct formation obtained by the corresponding benzyl alcohol and macrocycle at infinite distance.

Interestingly, although the conformation of macrocycles in the two complexes is similar, the formation of the **Bn$_3$TACN/Alcohol** is less favoured by 1.2 kcal mol^{-1} than that of **Me$_3$TACN/Alcohol**. From a deeper geometry analysis, it is shown that steric repulsion between the *N*-benzyl substituents and the macrocycle's backbone pushes the –CH$_2$ -benzyl side chains closer to the alcohol's –CH$_2$–, slightly destabilizing the complex (compare dihedral angles and –CH$_2$–···–CH$_2$– distances of the geometries in Fig. 8).

To reduce this steric interaction, the alcohol moves away from the nitrogen atoms (compare the distances N···H–O for **Me$_3$TACN/Alcohol** and for **Bn$_3$TACN/Alcohol** reported in

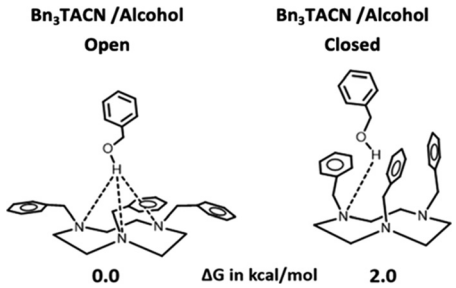


Fig. 7 The investigated geometries and relative free energy of **Bn$_3$TACN/Alcohol** complexes. The calculated distances between the three N atoms along with the alcohol proton are 2.12, 2.77 and 2.40 Å for the open geometry and 1.88, 3.14 and 3.16 Å for the close geometry.

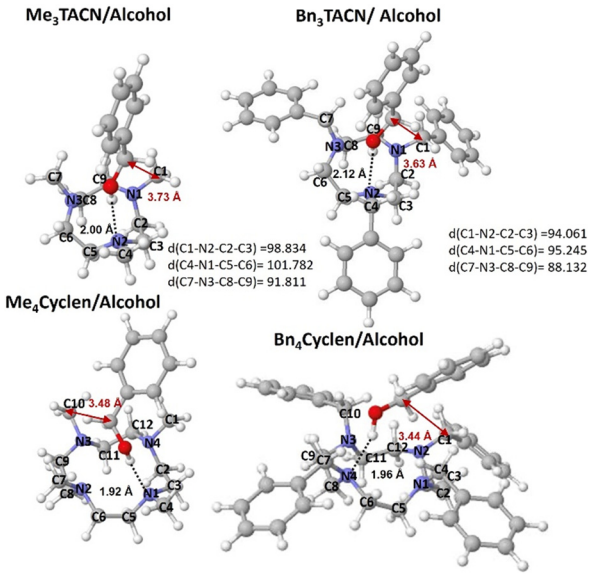


Fig. 8 Comparison of the **Me$_3$TACN/Alcohol**, **Bn$_3$TACN/Alcohol**, **Me$_4$cyclen/Alcohol**, **Bn$_4$cyclen/Alcohol** structures. For **Me$_3$TACN/Alcohol** and **Bn$_3$TACN/Alcohol** the values of the main dihedral angles (*d*) are reported.

Table S2 and Fig. S15†), and consequently the activation of the oxygen of the benzyl alcohol should be less favoured for the **Bn$_3$TACN/Alcohol** complex compared to the **Me$_3$TACN/Alcohol** one, with the latter bearing the less encumbered methyl substituents.

The distortion energies (ΔE kcal mol^{-1})[29] calculated for the formation of the adduct show that no important geometric deformations are generated (the ΔE is less than 1 kcal mol^{-1}), confirming that in the case of **Bn$_3$TACN** the alcohol is less well accommodated within the macrocycle for steric reasons and therefore interacts less effectively with the nitrogen atoms. As confirmation, the Mulliken population analysis performed on these complexes (see Table 2) shows a greater negative charge on the oxygen atom for **Me$_3$TACN/Alcohol** compared to **Bn$_3$TACN/Alcohol**, in line with the higher experimental activity of the former.[21,27,35]

Moving to cyclen derivatives, we performed calculations on **Me$_4$cyclen/Alcohol** and **Bn$_4$cyclen/Alcohol** complexes. As observed for **Bn$_3$TACN**, the conformation of **Bn$_4$cyclen** is different depending on whether it hosts a small cation ("closed" conformation)[36] or a larger neutral molecule as benzyl alcohol ("open" conformation).

In both the **Me$_4$cyclen/Alcohol** and **Bn$_4$cyclen/Alcohol** complexes the calculated geometries are compatible with the aforementioned cooperation of the nitrogen atoms (distances between the nitrogen atoms of 3.1 Å and angle values of 60° and 38°, for both adducts). Notably, the shorter OH···N distance in the case of tetrazamacrocycles, compared to the corresponding triazamacrocycles, (see Fig. S15†) agrees with their higher experimental activity.[21]

By comparing **Me$_4$cyclen/Alcohol** with **Bn$_4$cyclen/Alcohol**, calculations show that the methyl-substituted complex is

 This journal is © The Royal Society of Chemistry 2025

Open Access Article. Published on 27 September 2024. Downloaded on 1/28/2025 3:02:08 PM.
This article is licensed under a Creative Commons Attribution-NonCommercial 3.0 Unported Licence.

Table 2 Comparison of the Mulliken population analysis for the studied species. Mulliken charges on oxygen, hydrogen and nitrogen atoms

Species	Charge on O	Charge on H	Charge on N1, N2, N3, N4[a]
Alcohol	−0.275	0.173	
Me_3TACN/Alcohol	−0.321	0.215	−0.354, −0.319, −0.330
Bn_3TACN/Alcohol	−0.313	0.216	−0.324, −0.311, −0.341
Me_4cyclen/Alcohol	−0.337	0.199	−0.353, −0.316, −0.299, −0.312
Bn_4cyclen/Alcohol	−0.334	0.206	−0.350, −0.306, −0.298, −0.307

[a] Values related to **Me_4cyclen/Alcohol** and **Bn_4cyclen/Alcohol**.

about 1 kcal mol^{-1} more stable than the benzyl-substituted one for the same steric reasons discussed for the TACN analogues (see Fig. S15†). Consequently, for **Me_4cyclen/Alcohol** the N···H–O interaction is more effective (see Tables 2 and S2†), leading a more negative charge on the corresponding alcohol oxygen, in agreement with the greater activity observed experimentally.

Interestingly, by comparing the ΔG of formation of the triaza- and tetraza-macrocyles complexes with benzyl alcohol, it emerges that the **Me_4cyclen/Alcohol** and **Bn_4cyclen/Alcohol** are more favored than **Me_3TACN/Alcohol** by 2.3 and 1.2 kcal mol^{-1}, respectively. Interestingly, the calculated distortion energy is almost zero for both complexes, indicating that no deformation of the macrocycles in the interaction with the alcohol occurs.

Accordingly, the O–H···N distance decreases from 2.00 to 1.96 and to 1.92 Å moving from **Me_3TACN/Alcohol** to **Bn_4cyclen/Alcohol** and **Me_4cyclen/Alcohol**, respectively (Table 3), and the Mulliken population analysis also shows a greater negative charge on the oxygen for both **Me_4cyclen/Alcohol** and **Bn_4cyclen/Alcohol** when compared to **Me_3TACN/Alcohol** (see Tables 2 and S2† and Fig. 8). In conclusion, these results agree with the higher experimental activity observed for macrocycles with methyl substituents compared to macrocycles with benzyl substituents, as well as with the higher experimental activity observed for the **Me_4cyclen/Alcohol** and **Bn_4cyclen/Alcohol** compared with that of the analogous N_3 co-initiators.

Since both the calculations and the experimental results suggest that the activation of benzyl alcohol is affected by both the size of the macrocycle and the nature of its substituents, we decided to perform calculations on the six-membered complex **Bn_6hexacyclen/Alcohol** in an attempt to rationalize the unexpected inactivity of **Bn_6hexacyclen** in the L-lactide polymerization.

Interestingly, from the analysis of the optimized geometry of the macrocycle alone, it is shown that the conformation of **Bn_6hexacyclen** is not compatible with the demanded nitrogen atom cooperation for the alcohol activation, since the N–N distances are equal to 3.82 Å and the angle values are 96° and 25° (see Fig. 9). Therefore, to adopt the proper catalytically active conformation, **Bn_6hexacyclen** is forced to an unstable geometry. As a matter of fact, the energy of its complex with benzyl alcohol is approximately 3 kcal mol^{-1} from the reactants at infinite distance, with a macrocycle distortion energy of 1.2 kcal mol^{-1}.

A detailed analysis of the optimized geometry of the **Bn_6hexacyclen** macrocycle reveals that the nitrogen atoms are positioned alternately above and below the macrocycle plane and that the aromatic hydrogens interact with the N atoms stabilizing the structure (see Fig. 9A).

In the formation of the complex with the alcohol, one of these interactions is lost to be replaced by the hydrogen bond interaction with OH, leading to destabilization (see Fig. 9B).

Furthermore, whereas all *N*-substituents of TACN and cyclen derivatives are oriented out of the plane of the cycle; in the case of the **Bn_6hexacyclen** macrocycle, the substituents are approximately lying in the plane. Consequently, the benzyl substituents approach the nitrogen by interacting with the alcohol, crowding the catalytic space where the reaction with the monomer will take place. This could make the reaction less kinetically favoured for steric reasons (see Fig. 9B), in line with experimental kinetics studies, suggesting the participation of both thiourea and macrocycle in the decisive rate determining transition state.

Moreover, we believe that additional factors may contribute to the reduced catalytic activity in presence of **Bn_6hexacyclen**. Since thiourea can compete with alcohol in forming a host–guest complex with the macrocycles, thus

Table 3 Comparison of the O–H···N computed distances for **Me_3TACN/Alcohol**, **Bn_3TACN/Alcohol**, **Me_4cyclen/Alcohol** and **Bn_4cyclen/Alcohol** adducts

Adducts	O–H···N1 in Å	O–H···N2 in Å	O–H···N3 in Å	O–H···N4 in Å
Me_3TACN/Alcohol	2.00	2.45	2.85	
Bn_3TACN/Alcohol	2.12	2.40	2.77	
Me_4cyclen/Alcohol	1.92	2.73	2.99	3.93
Bn_4cyclen/Alcohol	1.96	2.75	2.86	3.82

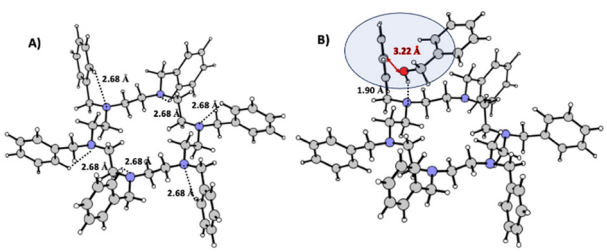


Fig. 9 Structures of A) the **Bn_6hexacyclen** macrocycle and B) the **Bn_6hexacyclen/Alcohol** complex.

Open Access Article. Published on 27 September 2024. Downloaded on 1/28/2025 3:02:08 PM.
This article is licensed under a Creative Commons Attribution-NonCommercial 3.0 Unported Licence.

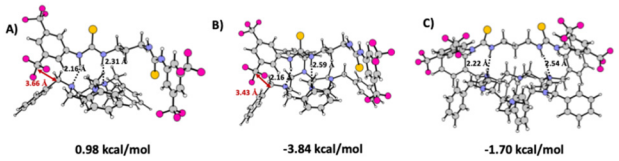


Fig. 10 Gibbs energy of the adduct formation obtained by A) **Bn$_3$TACN/bTU**, B) **Bn$_4$cyclen/bTU**, and C) **Bn$_6$hexacyclen/bTU** macrocycle at infinite distance.

deactivating the reaction, we conducted energy calculations for the formation **Bn$_3$TACN/bTU**, **Bn$_4$cyclen/bTU**, and **Bn$_6$hexacyclen/bTU** (see Fig. 10).

Interestingly, all three macrocycles form thermodynamically more favorable complexes with thiourea than with benzyl alcohol. Notably, the **Bn$_6$hexacyclen/bTU** complex is approximately 2 kcal mol^{-1} more stable than the corresponding **Bn$_3$TACN/bTU** and **Bn$_4$cyclen/bTU** complexes (compare the free energies of formation for the macrocycle/bis-thiourea complexes reported in Fig. 10 with the corresponding free energies of formation for macrocycle/alcohol complexes reported in Fig. 6, **Bn$_3$TACN/Alcohol**, **Bn$_4$cyclen/Alcohol**, and **Bn$_6$hexacyclen/Alcohol**). This result adds another piece to the overall picture of understanding the experimentally observed inactivity with **Bn$_6$hexacyclen**.

To summarize, **Bn$_6$hexacyclen** shows a conformation not compatible with the activation of the benzyl alcohol involving the cooperation of more nitrogen atoms. In fact, the energy formation of the complex with benzyl alcohol is higher than that observed for the corresponding triaza- and tetraza-derivatives by 2–3 kcal mol^{-1}, due to both the distortion of the macrocycle in the complex and the loss of a favourable interaction between the benzyl *ortho*-hydrogen and the adjacent nitrogen atom of the macrocycle. Moreover, the presence of the benzyl rings in the plane of the macrocycle suggests that the reaction between the alcohol and monomer could be kinetically unfavoured for steric reasons. Finally, the high stability of the host–guest macrocycle–thiourea complex sequesters both the catalytic components making them hardly available for the interaction with the alcohol and the L-lactide, respectively.

The combination of all these factors could explain the lack of catalytic activity experimentally observed for the **Bn$_6$hexacyclen** macrocycle.

Conclusions

In this work, we report new metal-free catalytic systems for the ring-opening polymerization of L-lactide, formed by a bis-thiourea and conformationally flexible cyclic polyamines with diverse sizes and *N*-substituents.

The polymerization data showed that the catalytic performance of these binary systems is dramatically affected by the structure of the macrocyclic polyamines. In particular, the tetrameric cyclen derived macrocycles were more active than traditionally employed trimeric ones, while the hexameric cyclic polyamine was completely inactive. In addition, *N*-methyl substituted polyaza-macrocycles were more efficient than the related *N*-benzyl substituted ones.

DFT calculations rationalized these results, demonstrating that the steric aspects are predominant for the activation of the alcohol by the macrocyclic polyamines. In fact, sterically bulkier substituents at the nitrogen atoms hamper the accessibility of the macrocycle's coordinative niche to the hydroxyl group of the alcohol/growing chains.

In trimeric and tetrameric polyaza-macrocycles, the proper distance between the nitrogen atoms allows their cooperation in the activation of the alcohol hydroxyl proton, that is significantly more efficient when compared to the larger cyclen derivatives.

Differently, for the hexacyclen macrocycle, the most stable conformation does not allow the cooperation of the nitrogen atoms in the activation of the benzyl alcohol. Moreover, a strong interaction between the macrocycle and the thiourea competes with the activation of the alcohol contributing to the inefficiency of the **Bn$_6$hexacyclen** cycle.

All the catalytic systems active in the ROP of L-lactide revealed a very good control of the polymerization reactions, as neglectable narrowly dispersed polymers of predictable molecular weights were obtained.

In conclusion, cyclic polyamines proved to be useful model compounds for the comprehension of the architectural characteristic of catalysts enabling cooperative activation of the substrates in the ROP polymerization and analogous organocatalyzed reactions. Considering their facile synthesis and the catalytic efficiency, cyclen derivatives have promise to be convenient organocatalysts, as an alternative to the well-established TACN derivatives, in the preparation of polylactide and other biodegradable polyesters.

Data availability

The data supporting this article have been included as part of the ESI.†

Author contributions

Conceptualization: G. D. S. and M. M.; methodology: A. D., M. V., F. B. and S. D.; investigation: F. D. R. and I. I.; visualization: F. D. R. and I. I.; data curation: M. M. and L. C.; writing – review and editing: M. M., G. D. S. and L. C. All authors have read and agreed to the published version of the manuscript.

Conflicts of interest

There are no conflicts to declare.

Acknowledgements

The authors thank Dr Federica Santulli for some synthetic work, Dr. Patrizia Iannece for MALDI-ToF analysis, Dr. Patrizia Oliva for NMR technical assistance and Dr. Mariagrazia Napoli for

 This journal is © The Royal Society of Chemistry 2025

Open Access Article. Published on 27 September 2024. Downloaded on 1/28/2025 3:02:08 PM.
This article is licensed under a Creative Commons Attribution-NonCommercial 3.0 Unported Licence.

GPC analysis. Financial support from the University of Salerno (FARB), and from PRIN 2020: "Natural Products-Assisted Organic Synthesis" (2020AEX4TA) is acknowledged.

Notes and references

1 A. Khalil, S. Cammas-Marion and O. Coulembier, *J. Polym. Sci., Part A: Polym. Chem.*, 2019, **57**, 657–672.
2 S. Liu, C. Ren, N. Zhao, Y. Shen and Z. Li, *Macromol. Rapid Commun.*, 2018, **39**, 1800485.
3 H. Wang, Z. Yao, Z. Li, Y. Zhu, C. Zhang, Z. Luo, T. Guo, Y. Gao, L. Zhang and K. Guo, *Eur. Polym. J.*, 2020, **127**, 109570.
4 D. Zhang, S. K. Boopathi, N. Hadjichristidis, Y. Gnanou and X. Feng, *J. Am. Chem. Soc.*, 2016, **138**, 11117–11120.
5 M. Alves, B. Grignard, R. Mereau, C. Jerome, T. Tassaing and C. Detrembleur, *Catal. Sci. Technol.*, 2017, **7**, 2651–2684.
6 F. Nederberg, B. G. G. Lohmeijer, F. Leibfarth, R. C. Pratt, J. Choi, A. P. Dove, R. M. Waymouth and J. L. Hedrick, *Biomacromolecules*, 2007, **8**, 153–160.
7 B. Han, L. Zhang, B. Liu, X. Dong, I. Kim, Z. Duan and P. Theato, *Macromolecules*, 2015, **48**, 3431–3437.
8 L. Lin, J. Liang, Y. Xu, S. Wang, M. Xiao, L. Sun and Y. Meng, *Green Chem.*, 2019, **21**, 2469–2477.
9 S. Pappuru and D. Chakraborty, *Eur. Polym. J.*, 2019, **121**, 109276.
10 J. Zhang, L. Wang, S. Liu and Z. Li, *J. Polym. Sci.*, 2020, **58**, 803–810.
11 D. Ryzhakov, G. Printz, B. Jacques, S. Messaoudi, F. Dumas, S. Dagorne and F. Le Bideau, *Polym. Chem.*, 2021, **12**, 2932–2946.
12 W. Zhao, Y. Gnanou and N. Hadjichristidis, *Polym. Chem.*, 2015, **6**, 6193.
13 M. K. Kiesewetter, E. J. Shin, J. L. Hedrick and R. M. Waymouth, *Macromolecules*, 2010, **43**, 2093–2107.
14 M. Valle, M. Ximenis, X. Lopez de Pariza, J. M. W. Chan and H. Sardon, *Angew. Chem., Int. Ed.*, 2022, **61**, e202203043.
15 W. N. Ottou, H. Sardon, D. Mecerreyes, J. Vignolle and D. Taton, *Prog. Polym. Sci.*, 2016, **56**, 64–115.
16 M. E. G. Mosquera, M. Palenzuela and M. Fernández-Millán, in *Noncovalent Interactions in Catalysis*, ed. K. T. Mahmudov, M. N. Kopylovich, M. F. C. Guedes da Silva and A. J. L. Pombeiro, The Royal Society of Chemistry, 2019, DOI: 10.1039/9781788016490-00415.
17 F. Nederberg, E. F. Connor, M. Moeller, T. Glauser and J. L. Hedrick, *Angew. Chem., Int. Ed.*, 2001, **40**, 2712–2715.
18 N. E. Kamber, W. Jeong, R. M. Waymouth, R. C. Pratt, B. G. G. Lohmeijer and J. L. Hedrick, *Chem. Rev.*, 2007, **107**, 5813–5840.
19 S. Hu, J. Zhao, G. Zhang and H. Schlaad, *Prog. Polym. Sci.*, 2017, **74**, 34–77.
20 P. Olsén, K. Odelius, H. Keul and A.-C. Albertsson, *Macromolecules*, 2015, **48**, 1703–1710.
21 B. G. G. Lohmeijer, R. C. Pratt, F. Leibfarth, J. W. Logan, D. A. Long, A. P. Dove, F. Nederberg, J. Choi, C. Wade, R. M. Waymouth and J. L. Hedrick, *Macromolecules*, 2006, **39**, 8574–8583.
22 B. Lin and R. M. Waymouth, *Macromolecules*, 2018, **51**, 2932–2938.
23 L. Zhang, R. C. Pratt, F. Nederberg, H. W. Horn, J. E. Rice, R. M. Waymouth, C. G. Wade and J. L. Hedrick, *Macromolecules*, 2010, **43**, 1660–1664.
24 R. C. Pratt, B. G. G. Lohmeijer, D. A. Long, R. M. Waymouth and J. L. Hedrick, *J. Am. Chem. Soc.*, 2006, **128**, 4556–4557.
25 B. Lin and R. M. Waymouth, *J. Am. Chem. Soc.*, 2017, **139**, 1645–1652.
26 I. Jain and P. Malik, *Eur. Polym. J.*, 2020, **133**, 109791.
27 N. U. Dharmaratne, J. U. Pothupitiya and M. K. Kiesewetter, *Org. Biomol. Chem.*, 2019, **17**, 3305–3313.
28 K. Makiguchi, T. Yamanaka, T. Kakuchi, M. Terada and T. Satoh, *Chem. Commun.*, 2014, **50**, 2883–2885.
29 L. Zhang, F. Nederberg, R. C. Pratt, R. M. Waymouth, J. L. Hedrick and C. G. Wade, *Macromolecules*, 2007, **40**, 4154–4158.
30 O. Coulembier, A. P. Dove, R. C. Pratt, A. C. Sentman, D. A. Culkin, L. Mespouille, P. Dubois, R. M. Waymouth and J. L. Hedrick, *Angew. Chem., Int. Ed.*, 2005, **44**, 4964–4968.
31 M. Fevre, J. Pinaud, Y. Gnanou, J. Vignolle and D. Taton, *Chem. Soc. Rev.*, 2013, **42**, 2142–2172.
32 E. F. Connor, G. W. Nyce, M. Myers, A. Moeck and J. L. Hedrick, *J. Am. Chem. Soc.*, 2002, **124**, 914–915.
33 C. Thomas and B. Bibal, *Green Chem.*, 2014, **16**, 1687–1699.
34 S. S. Spink, O. I. Kazakov, E. T. Kiesewetter and M. K. Kiesewetter, *Macromolecules*, 2015, **48**, 6127–6131.
35 D. J. Coady, A. C. Engler, H. W. Horn, K. M. Bajjuri, K. Fukushima, G. O. Jones, A. Nelson, J. E. Rice and J. L. Hedrick, *ACS Macro Lett.*, 2012, **1**, 19–22.
36 R. Schettini, A. D'Amato, G. Pierri, C. Tedesco, G. Della Sala, O. Motta, I. Izzo and F. De Riccardis, *Org. Lett.*, 2019, **21**, 7365–7369.
37 K. V. Fastnacht, S. S. Spink, N. U. Dharmaratne, J. U. Pothupitiya, P. P. Datta, E. T. Kiesewetter and M. K. Kiesewetter, *ACS Macro Lett.*, 2016, **5**, 982–986.
38 J. P. Perdew, *Phys. Rev. B*, 1986, **33**, 8822.
39 J. P. Perdew, *Phys. Rev. B*, 1986, **34**, 7406.
40 A. D. Becke, *Phys. Rev. A*, 1988, **38**, 3098.
41 M. J. Frisch, G. W. Trucks, H. B. Schlegel, G. E. Scuseria, M. A. Robb, J. R. Cheeseman, G. Scalmani, V. Barone, B. Mennucci, G. A. Petersson, H. Nakatsuji, M. Caricato, X. Li, H. P. Hratchian, A. F. Izmaylov, J. Bloino, G. Zheng, J. L. Sonnenberg, M. Hada, M. Ehara, K. Toyota, R. Fukuda, J. Hasegawa, M. Ishida, T. Nakajima, Y. Honda, O. Kitao, H. Nakai, T. Vreven, J. A. Montgomery, J. E. Peralta, F. Ogliaro, M. Bearpark, J. J. Heyd, E. Brothers, K. N. Kudin, V. N. Staroverov, R. Kobayashi, J. Normand, K. Raghavachari, A. Rendell, J. C. Burant, S. S. Iyengar, J. Tomasi, M. Cossi, N. Rega, J. M. Millam, M. Klene, J. E. Knox, J. B. Cross, V. Bakken, C. Adamo, J. Jaramillo, R. Gomperts, R. E. Stratmann, O. Yazyev, A. J. Austin, R. Cammi, C. Pomelli, J. W. R. Ochterski, L. Martin, K. Morokuma, V. G. Zakrzewski, G. A. Voth, P. Salvador, J. J. Dannenberg, S. Dapprich, A. D. Daniels, Ö. Farkas, J. B. Foresman, J. V. Ortiz, J. Cioslowski and D. J. Fox, *Gaussian 09 Revision A.1*, Gaussian, Inc., Wallingford, CT, 2009.

Open Access Article. Published on 27 September 2024. Downloaded on 1/28/2025 3:02:08 PM.
This article is licensed under a Creative Commons Attribution-NonCommercial 3.0 Unported Licence.

42 M. M. Francl, W. J. Pietro, W. J. Hehre, J. S. Binkley, D. J. DeFrees, J. A. Pople and M. S. Gordon, *J. Chem. Phys.*, 1982, **77**, 3654–3665.
43 V. Barone and M. Cossi, *J. Phys. Chem. A*, 1998, **102**, 1995–2001.
44 J. Tomasi and M. Persico, *Chem. Rev.*, 1994, **94**, 2027–2094.
45 Y. Zhao and D. G. Truhlar, *Theor. Chem. Acc.*, 2008, **120**, 215–241.
46 A. Schaefer, C. Huber and R. Ahlrichs, *J. Chem. Phys.*, 1994, **100**, 5829–5835.
47 S. Grimme, S. Ehrlich and L. Goerigk, *J. Comput. Chem.*, 2011, **32**(7), 1456–1465.
48 R. Schettini, A. D'Amato, A. M. Araszczuk, G. Della Sala, C. Costabile, A. M. D'Ursi, M. Grimaldi, I. Izzo and F. De Riccardis, *Org. Biomol. Chem.*, 2021, **19**, 7420–7431.
49 A. M. Araszczuk, G. Pierri, R. Schettini, C. Costabile, G. Della Sala, L. Di Marino, C. Tedesco, F. De Riccardis and I. Izzo, *Chem. – Eur. J.*, 2024, **30**, e202400904.
50 J. Wallick, C. G. Riordan and G. P. A. Yap, *J. Am. Chem. Soc.*, 2013, **135**, 14972–14974.
51 E. Evangelio, N. P. Rath and L. M. Mirica, *Dalton Trans.*, 2012, **41**, 8010–8021.
52 X.-Q. Xiong, F. Liang, L. Yang, X.-L. Wang, X. Zhou, C.-Y. Zheng and X.-P. Cao, *Chem. Biodiversity*, 2007, **4**, 2791–2797.
53 A. P. Dove, R. C. Pratt, B. G. G. Lohmeijer, R. M. Waymouth and J. L. Hedrick, *J. Am. Chem. Soc.*, 2005, **127**, 13798–13799.
54 R. C. Pratt, B. G. G. Lohmeijer, D. A. Long, P. N. P. Lundberg, A. P. Dove, H. Li, C. G. Wade, R. M. Waymouth and J. L. Hedrick, *Macromolecules*, 2006, **39**, 7863–7871.
55 G. Tárkányi, P. Király, T. Soós and S. Varga, *Chem. – Eur. J.*, 2012, **18**, 1918–1922.
56 R. C. Pratt, B. G. G. Lohmeijer, D. A. Long, P. N. P. Lundberg, A. P. Dove, H. Li, C. G. Wade, R. M. Waymouth and J. L. Hedrick, *Macromolecules*, 2006, **39**, 7863.

 This journal is © The Royal Society of Chemistry 2025